

The sealing mechanism of radial lip seals: A numerical study of the tangential distortion of the sealing edge

Jeremias GRÜN ^{*}, Simon FELDMETH , Frank BAUER 

University of Stuttgart – Institute of Machine Components, Stuttgart, Germany

*Corresponding author: jeremias.gruen@ima.uni-stuttgart.de

Keywords

radial lip seal
finite element analysis
surface roughness
elastic deformation
elastomers

History

Received: 21-01-2022

Revised: 10-03-2022

Accepted: 18-03-2022

Abstract

The sealing behaviour of elastomeric radial lip seals is essentially affected by the sealing mechanism in the contact area between the sealing edge and the shaft surface. The relative motion between radial lip seal and shaft deforms the sealing edge tangentially in the circumferential direction. This mechanical deformation is considered essential for the sealing mechanism. In this study, a numerical approach is employed to simulate this deformation. A three-dimensional multiscale model serves this purpose. The radial lip seal geometry is described on the macro-scale. On the micro-scale, an artificial rough surface with a stochastic roughness distribution is applied to an ideal sealing edge surface. A new meshing algorithm is used to discretise different sealing edge surfaces and automatically generates structured hexahedral meshes of the sealing edges. Mesh transitions connect the resulting finely meshed sealing edge to the coarsely meshed global macro-scale mesh of the radial lip seal. The paper introduces the modelling method used to simulate the deformation of radial lip seals. Results are presented and discussed with reference to the sealing behaviour. This contributes to a better understanding of the sealing mechanism of radial lip seals.

1. Introduction

For decades, elastomeric radial lip seals according to [1] and [2] have been used to seal shaft passages in many mechanical and automotive engineering applications. Bauer [3] and Bauer and Haas [4] provide an overview of the function of radial lip seals. Figure 1a shows a radial lip seal in schematic form. The sealing ring, along with the shaft counter face, the fluid to be sealed, as well as the ambient and operating conditions, constitutes the complex tribological system radial lip seal. Radial lip seals prevent fluid from leaking into the environment (air side). They keep dirt and dust from entering the area to be sealed (fluid side). Under static conditions, the sealing edge is pressed onto the shaft by the interference between the inner diameter of the sealing ring and the outer diameter of the shaft and the spring

load. This prevents the exchange of fluid between the environment and the area to be sealed. During operation, the shaft drags fluid between the sealing edge and the shaft surface. This creates a thin lubricant film in the sealing gap. Additionally, fluid entering the sealing gap is pumped back from the air side to the fluid side. Consequently, the radial lip seal is dynamically leak-tight. Although this effect has been observed for years, it is still not completely understood.

The most common physical operating principles and functional hypotheses explaining the lubrication and sealing mechanism of radial lip seals are summarised by Bauer [3]. One of the most promising principles is the sealing edge distortion principle assumed by Kammüller and Müller [5,6]. Kawahara et al. [7,8] observed the sealing contact through a hollow glass shaft. They found a friction dependent tangential deformation of the sealing edge surface. This deformation is identified as the cause of the sealing mechanism. Kammüller [5] showed the correlation between

tangential distortions and pumping capability. Back pumping capable radial lip seals show asymmetrical distortions. Radial lip seals without back pumping capability show symmetrical distortions. Kammüller [5] attributed this to the sealing edge geometry and the resulting contact pressure distribution. He derived the sealing edge distortion principle shown in Figure 1b on this basis. The asperities on the rough sealing edge surface are compressed during mounting (a). The relative motion between the shaft and sealing edge surfaces induces shear stresses (b), causing a tangential distortion of the asperities (c). The distorted asperities deflect the tangential fluid flow in the axial direction. This results in the two oppositely directed fluid flows \dot{m}_{bp} and \dot{m}_k in the axial direction (d). Because of the asymmetrical distortion, the fluid flow to the air side (leakage) \dot{m}_k is less than the back-pumping flow to the fluid side \dot{m}_{bp} . Therefore, the resulting flow rate \dot{m}_{pr} is directed axially towards the fluid side. The radial lip seal is consequently leak-tight.

This effect could be confirmed by visual observations by van Leeuwen et al. [10] and Schulz et al. [11]. Although the tangential distortions could be observed, a direct correlation to the pressure distribution could not be established. Numerical analyses provide a further approach to the investigation of the structural-mechanical effects in the sealing contact. This allows a targeted analysis of the different influences on the sealing mechanism. In contrast to test rig experiments, numerical analyses are not affected by external disturbances. In earlier work, Stakenborg et al. [12,13] studied the mounting process of radial lip seals, i.e. the radial deformation of the sealing edge, using ideal two-

dimensional models. This allowed them to analyse the pressure distribution in the axial direction. Tønder and Salant [14] and Salant and Flaherty [15,16] approximated the sealing edge roughness by axial striations, micro undulations and circular asperities. Based on this, Salant [17] developed an elasto-hydrodynamic model of the lubricant film and a simplified model of the meniscus on the air side of the sealing edge. Thus, he was able to predict the sealing behaviour of radial lip seals. Salant and Rocke [18] utilised mathematical expressions to describe the tangential displacement of these idealised surface patterns. Di Benedetto et al. [19] combined these approaches to predict the lubricant film thickness of radial lip seals. Wenk et al. [20] used a three-dimensional model to examine the radial deformation of rough sealing edges during mounting. The model included real measured rough sealing edge surfaces. Tangential deformations caused by the shaft rotation were not considered. The present paper shows a numerical approach to simulate the contact mechanics in the sealing contact in the radial and circumferential direction. The present paper aims to fill the gap between theoretical [5-8], numerical considerations [12-16,18-20] and visual observations [10,11]. A three-dimensional multiscale model serves this purpose, as in [20]. This enables a realistic rough sealing edge surface to be implemented. In addition to the radial compression, the tangential distortion of the sealing edge caused by the shaft rotation is simulated. This allows a direct correlation to be established between the radial contact pressure and the tangential distortion of the sealing edge surface.

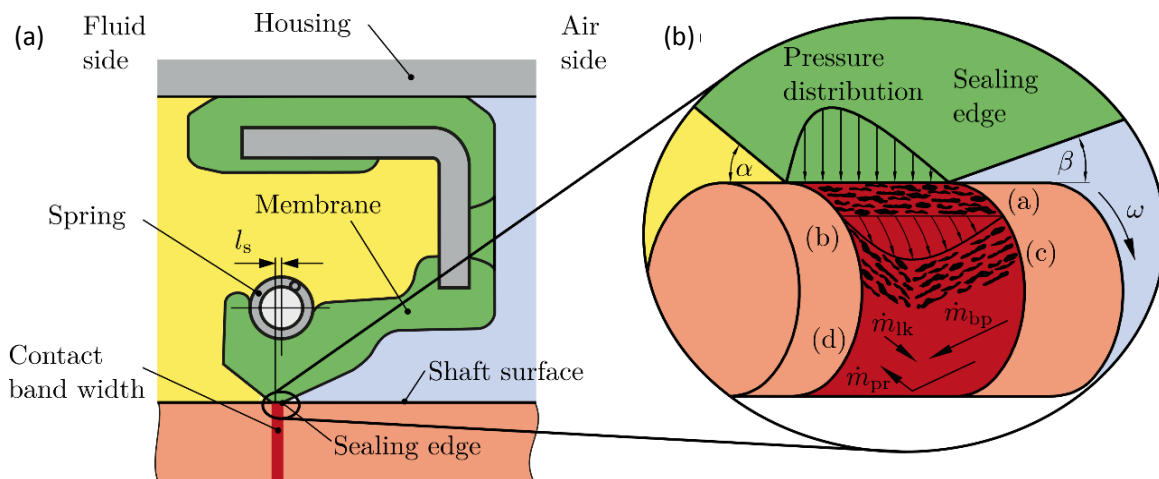


Figure 1. Radial lip seal (a) and sealing edge distortion principle (b). Reprinted from [9] with permission from Elsevier

2. Methods

A widely used method for simulating structural mechanic problems is finite element analysis (FEA). The modelling is one of the most decisive aspects of this method. Before modelling, it is necessary to specify which effects must be investigated and which can be neglected. In this paper, both macroscopic and microscopic structural mechanic effects in sealing contact are analysed. The following section deals with the numerical generation of rough sealing edge surfaces. An efficient meshing strategy is introduced. The material definition and boundary conditions applied are discussed.

2.1 Numerical modelling of rough sealing edge surfaces

The sealing edge distortion principle [5] is essentially based on the microscopic effects in the sealing contact. Thus, the roughness of the sealing edge must be considered in the numerical analyses.

A stochastically rough surface $z = f(x, y)$ can be described by a height distribution function and an autocovariance function. The height distribution function indicates the deviation from a mean surface height. The autocovariance function characterizes the lateral distribution of asperities across the surface. Following [21,22], it is assumed that both functions are Gaussian distributed. The height distribution function is given by

$$h(f(x, y)) = \frac{1}{\sqrt{2\pi\sigma^2}} e^{-\frac{f^2(x, y)}{2\sigma^2}}, \quad (1)$$

where σ is the root mean square (RMS) height. The autocovariance function is given by

$$c(x, y) = e^{-\frac{x^2}{\lambda_x^2} - \frac{y^2}{\lambda_y^2}}, \quad (2)$$

where λ_x and λ_y are the correlation lengths in x and y direction. Garcia and Stoll [23] describe a method to generate rough surfaces numerically. Normally distributed random numbers are generated from discrete x and y values. The result is an uncorrelated Gaussian random rough surface distribution $f_u(x, y)$. For the correlation of the surface nodes the distribution is convolved with the Gaussian filter

$$F(x, y) = \frac{2(\Delta x + \Delta y)}{(n_x + n_y)\sqrt{\pi\lambda_x\lambda_y}} e^{-2\left(\frac{x^2}{\lambda_x^2} + \frac{y^2}{\lambda_y^2}\right)}. \quad (3)$$

Here Δx and Δy are the distances between the surface nodes in x and y direction, respectively. The m and n correspond to the number of surface nodes in x and y direction. This results in the correlated distribution

$$f(x, y) = \int \int_{-\infty}^{\infty} F(x-x', y-y') f_u(x', y') dx' dy'. \quad (4)$$

The implementation is done using a fast Fourier transformation algorithm as described in [24]. Figure 2 shows an isotropic rough surface generated by this method. The surface can easily be applied to an ideally smooth sealing edge surface. The result is a rough sealing edge surface as shown in Figure 3.

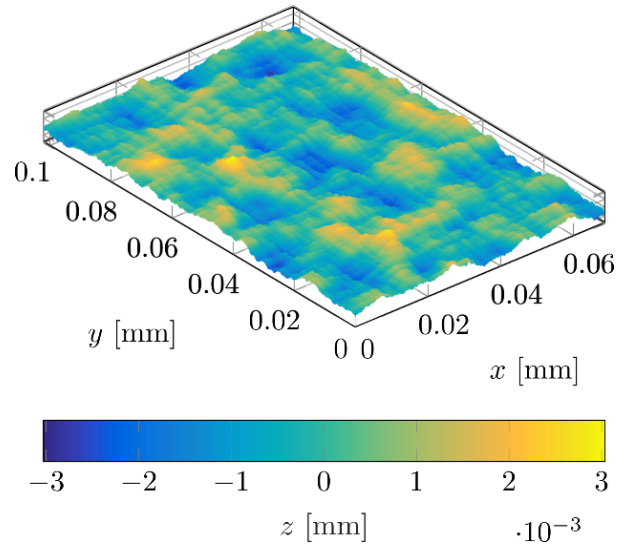


Figure 2. Numerically generated rough surface: $\sigma = 1.6 \mu\text{m}$, $\lambda_x = 10 \mu\text{m}$, $\lambda_y = 10 \mu\text{m}$

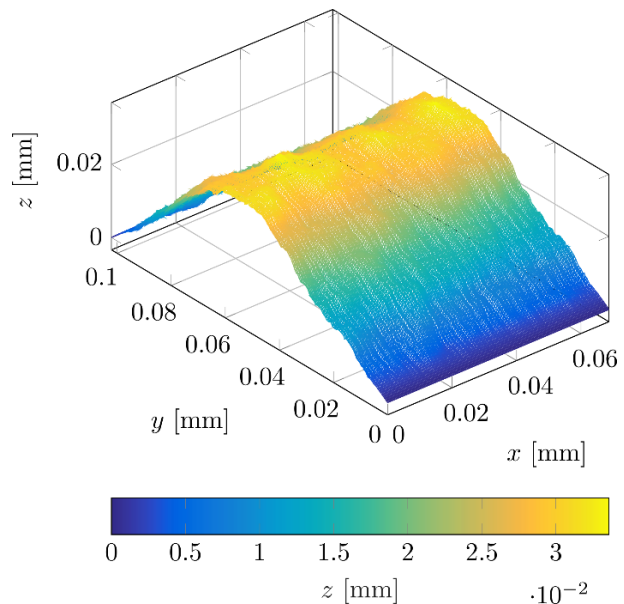


Figure 3. Rough sealing edge surface

2.2 FE meshing

The meshing of the computational domain represents a fundamental step in the FEA. The computational effort and the quality of the results are often in conflict. It is necessary to consider which effects should be investigated and what can be neglected. The housing, the upper part of the membrane and the metal insert are neglected in the following simulations. The shaft and the spring are considered as rigid bodies and therefore approximated as solid surfaces. To keep the calculation effort low, a rotational symmetric segment of the radial lip seal is simulated. The structural mechanics in the contact area between sealing edge and shaft surface are of particular interest. The FE mesh is therefore divided into two subdomains as shown in Figure 4. The sealing edge (subdomain 1) is finely meshed. The mesh of the remaining sealing body of the radial lip seal (subdomain 2) is coarser meshed.

The mesh construction is based on [9]. An algorithm automatically meshes arbitrary sealing edge geometries (subdomain 1). The surface coordinates of the sealing edge geometry and the interface height h_{int} provide the input data. The surface coordinates can be obtained from CAD models as well as from topography measurements of real surfaces. Based on the recommendation of

[25] structured hexahedral FE meshes are used. Benzley et al. [25] were able to achieve more accurate results with hexahedral meshes for elastic and elasto-plastic analyses compared to tetrahedral meshes.

The sealing body (subdomain 2) is meshed with Altair HyperMesh [26]. The sealing edge (subdomain 1) is imported into HyperMesh and connected to the sealing body (subdomain 2) via the interface nodes. Figure 4 shows the mesh resolution of the subdomains is the same in the interface region. Starting from the interface region, the mesh coarsens via mesh transitions. The resulting mesh of the radial lip segment is shown in Figure 4. It consists of a total of ≈ 265.100 elements, of which ≈ 163.800 include the sealing edge alone. This corresponds to $\approx 63\%$ of the total number of elements and thus to a high mesh resolution in the decisive contact area (element edge length $\approx 1\ \mu\text{m}$). High accuracy is thus achieved at a reasonable computational effort. Furthermore, this mesh construction allows efficient analyses of various sealing edge geometries without changing the entire FE mesh.

2.3 Material properties and boundary conditions

The preprocessing and solving are done with MSC Marc/Mentat [27]. Figure 5 shows the FE

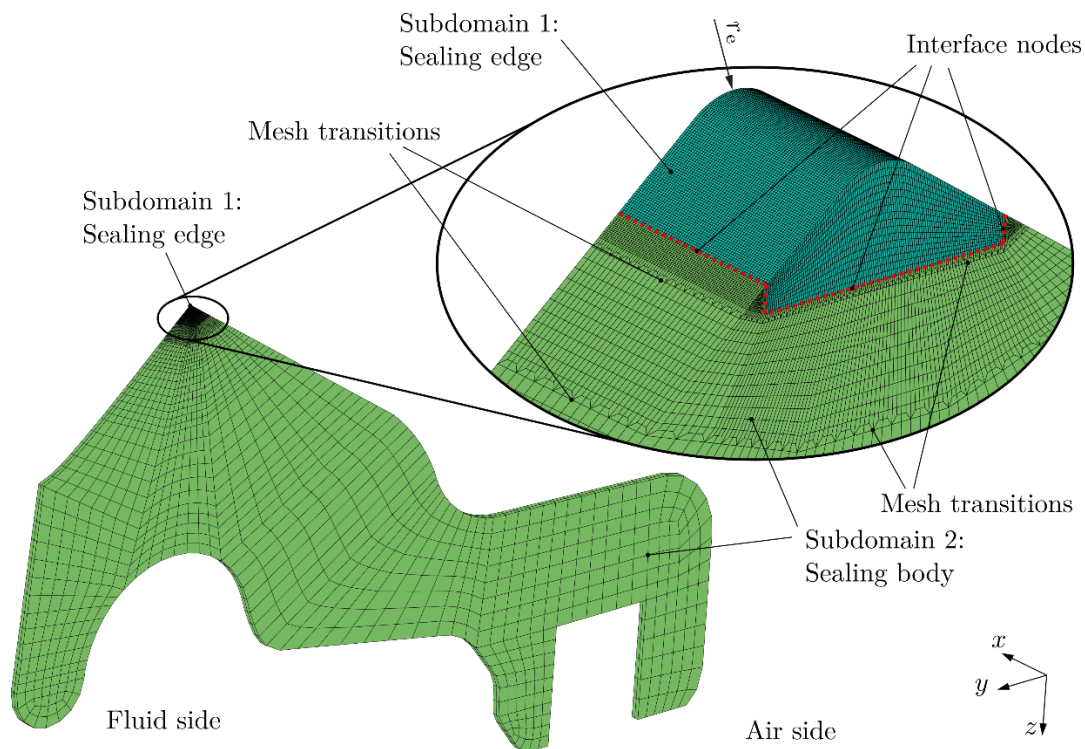


Figure 4. FE mesh of a radial lip seal segment

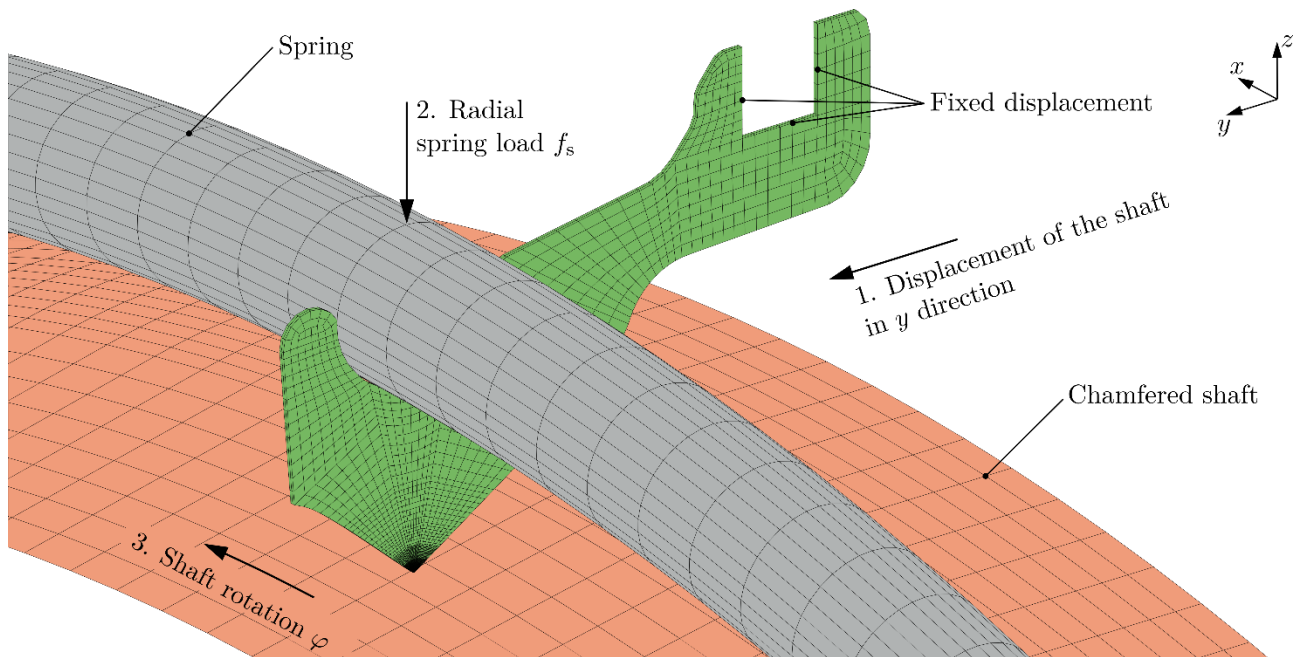


Figure 5. FE model of the radial lip seal segment. Reprinted from [9] with permission from Elsevier

model with the previously meshed radial lip seal segment. The element type used is an eight-node, isoparametric hexahedral element with trilinear interpolation functions. This element type is preferred for contact analyses according to [28]. A hyperelastic Neo-Hookean material model with the material parameter $C_{10} = 1.34$ MPa is applied. This corresponds to the material properties of a radial lip seal made of fluoro rubber (FKM). Feldmeth et al. [29] present methods for the determination of these parameters. Tasora et al. [30] present a different method for determining the material parameters of radial lip seals and for calibrating FE models. The shaft and the spring are modelled as surfaces and approximated as ideal rigid bodies. The shaft has a diameter of $d = 80$ mm. The contact between the spring and the membrane is assumed to be frictionless. Isotropic friction between the sealing edge and the shaft is modelled. The friction is modelled in a first approximation by a bilinear Coulomb friction model. The friction coefficient is varied in the range of $\mu = 0.20 \dots 0.35 \dots 0.50$. According to Johnston and Vogt [31] and Engelke [32], these friction coefficients are typical for a wide range of lubricants and elastomers. Plath et al. [33] compared measured data with simulation results for the friction torque of radial lip seals. They achieved comparable friction torque at a friction coefficient of $\mu = 0.35$. The node-to-segment algorithm of MSC Marc/Mentat is used

to solve the contact problem. A fixed displacement condition is applied at the joint between the sealing body and the metal insert, i.e. node displacements are locked in all directions. The spring load $f_s = 18$ N is approximated as a point load on a control node of the spring. The value for the spring load was determined by radial load measurements according to [34]. For this purpose, the radial load of the radial lip seal was first measured without the spring and subsequently with the mounted spring. The difference between the two values results in the spring load. The FE mesh is a 0.1° segment of the radial lip seal. Consequently, a cyclic boundary condition around the y axis is applied to the boundary nodes. The quasi-static simulation is divided into three load steps. The first load step is mounting the shaft. The shaft moves in the y direction, widening the radial lip seal. In the second load step, the spring load is applied. Compared to the real mounting process, these two load steps are reversed because the spring load acts before the shaft is shifted in. This does not affect the simulation, since the quasi-static approach does not take transient effects into account. However, the reversal of the two load steps improves the convergence behaviour. In the last load step, the shaft rotates around the y axis at an angle of $\varphi = 1$ rad. The simulation parameters and the methods and how they were determined are summarised in Table 1.

Table 1. Simulation parameters

Parameter	Value	Determination method
Material parameter C_{10} (FKM)	1.34 MPa	Tensile test [29]
Shaft diameter d	80 mm	–
Friction coefficient μ	0.20 ... 0.50	Literature [31-33]
Spring load f_s	18 N	Radial load measurements [34]
Rotation angle φ	1 rad	–
Sealing edge radius r_e	0.025 mm, 0.050 mm	Axle-sections [35]

3. Results

The following section describes the results of structural simulations of radial lip seals with different sealing edges. Based on the results of ideal smooth sealing edges, a rough sealing edge is studied and presented. The simulations are performed on an Intel Xeon CPU W-2155 @ 3.3 GHz with 128 GB of RAM. All models proved to be very robust and showed no convergence problems. Compared to the simulation time of ~ 18 h for the ideal smooth sealing edges, the simulation of the rough sealing edge takes ~ 32 h. This difference can be explained by the significantly more time-consuming contact analysis for the rough surface.

3.1 Ideal smooth sealing edges

Two ideal smooth sealing edges are analysed. The results provide the correlation between the contact behaviour, the contact pressure and the local tangential displacements. In reality, sealing edges are not absolutely sharp-edged. As illustrated in Figure 4, they always have a finite radius. This radius is varied in the following sealing edge analysis. One sealing edge has the radius $r_e = 0.025$ mm. The other one has the radius $r_e = 0.050$ mm. The geometry of the remaining radial lip seal is identical. The friction coefficient is initially $\mu = 0.35$.

The profiles of the compressed sealing edges h and the contact pressures p are shown in Figures 6 and 7. The curves are plotted in cross-section along the axis of rotation y . The h coordinate shows the compressed sealing edge profile in radial direction. The sealing edges considerably differ in the contact

widths. The sealing edge with the smaller radius has a smaller contact width. The smaller radius leads to a strong curvature. This causes the sealing edge not to contact as broad and the contact width is smaller. This effect is also visible from the contact pressure p . With the smaller sealing edge radius shown in Figure 6, the maximum contact pressure increases and the pressure is distributed over a smaller contact width. Figures 6 and 7 also show the influence of the asymmetry of the contact angles on the asymmetry of the pressure distribution. As the contact angle on the fluid side increases, the maximum of the pressure distribution shifts to the fluid side. If the contact angles equalize, a symmetrical pressure distribution is obtained.

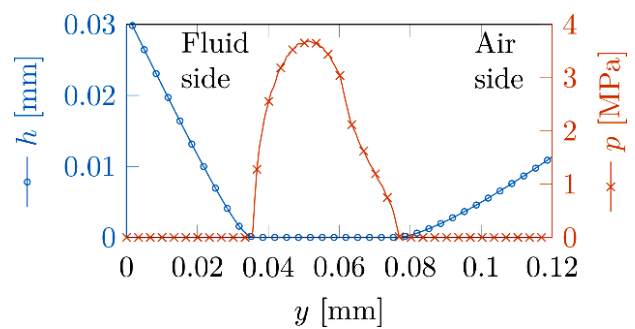


Figure 6. Cross-section of the deformed sealing edge and contact pressure profile: $r_e = 0.025$ mm

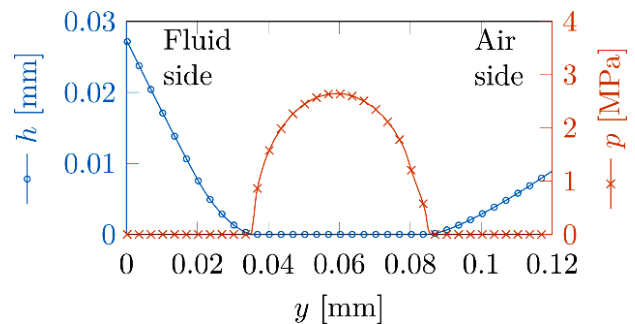


Figure 7. Cross-section of the deformed sealing edge and contact pressure profile: $r_e = 0.050$ mm

The shaft rotates at about an angle of $\varphi = 1$ rad which corresponds to a sliding distance of 40 mm. This distorts the sealing edge tangentially in the circumferential direction. The resulting displacements w are correlated with the pressure p in Figures 8 and 9. They show the direct contact area with the contact width b along the rotation axis. The pressure profile corresponds closely to the shape of the deformation distribution. The respective maxima of the pressure and the distortion curves are at the same position of the contact width. Moreover, the tangential deformation is larger on the fluid side than on the air side in case of asymmetrical pressure

distribution. These conclusions correspond with that of Kawahara et al. [7,8] and Kammüller [5].

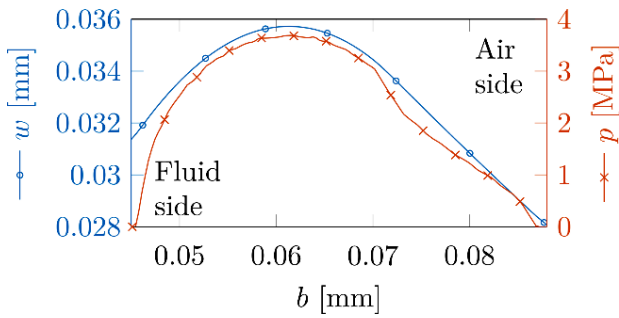


Figure 8. Tangential displacement and contact pressure: $r_e = 0.025$ mm

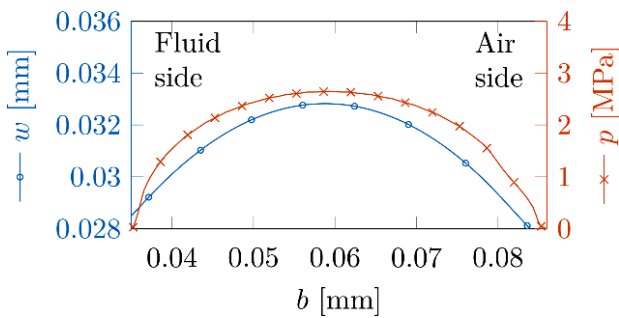


Figure 9. Tangential displacement and contact pressure: $r_e = 0.050$ mm

The influence of friction is evaluated using the sealing edge with a radius of $r_e = 0.025$ mm. For a better understanding, the terms tangential displacement w and tangential distortion u are distinguished in the following. The tangential displacement w describes the total displacement of the sealing edge. The tangential distortion u is defined as the displacement of the sealing edge relative to the minimum tangential displacement in the contact width b . Figure 10 shows the displacement w of the sealing edge at different friction coefficients μ . Figure 11 shows the distortion u of the sealing edge over the contact width b at different friction coefficients. Considering the displacement, the proportionality of the normal load (spring load f_s) and the tangential force over the friction coefficient μ is apparent. With an increase of the friction coefficient by an increment of $\Delta\mu = 0.05$, the displacement increases by $\sim 10\%$. Although the same increase in the friction coefficient leads to an increase in the maximum distortion, the distribution of the distortion remains similar.

3.2 Rough sealing edge

The rough sealing edge surface from section 2.1 is simulated. It has a macroscopic radius of $r_e = 0.025$ mm. The friction coefficient is again $\mu = 0.35$.

Figure 12 shows the mounted and Figure 13 the distorted unfolded surface of the rough sealing edge. The x axis corresponds to the circumferential direction and the y axis to the axis of rotation. The z coordinate and the colour bar represent the height of the deformed sealing edge. As shown in Figure 12 the sealing edge continuously contacts the shaft surface over the entire circumference after mounting. The radial lip seal is thus statically leak-tight. Due to the relative movement between the tangential and circumferential direction. This results in the directed microscopic back-pumping structures shown in Figure 13 which are considered essential for the pumping capability of radial lip seals.

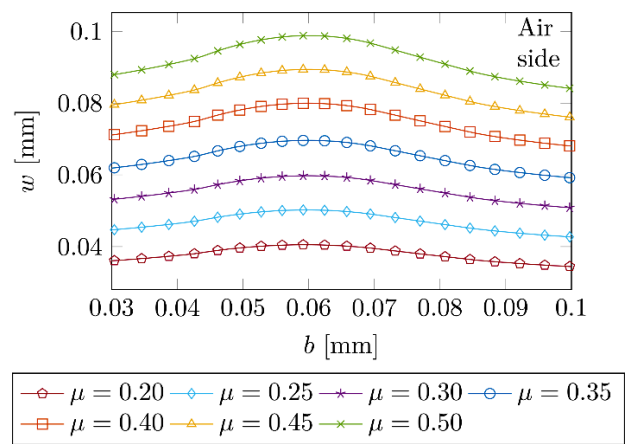


Figure 10. Tangential displacement w at different friction coefficients

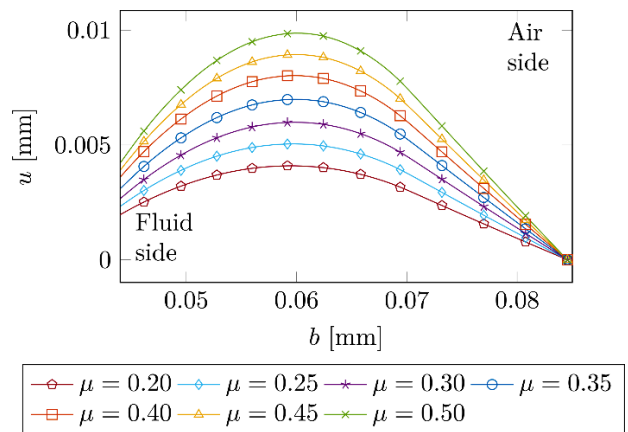


Figure 11. Tangential distortion u at different friction coefficients

The contour plots of the contact pressure in Figures 14 and 15 clarify the local tangential deformations. They show the pressure levels in the contact area. The pressure is distributed stochastically over the contact area. The pressure maximum is oriented towards the fluid side. The pressure distribution shows pressure peaks and valleys. After mounting, they are oriented in

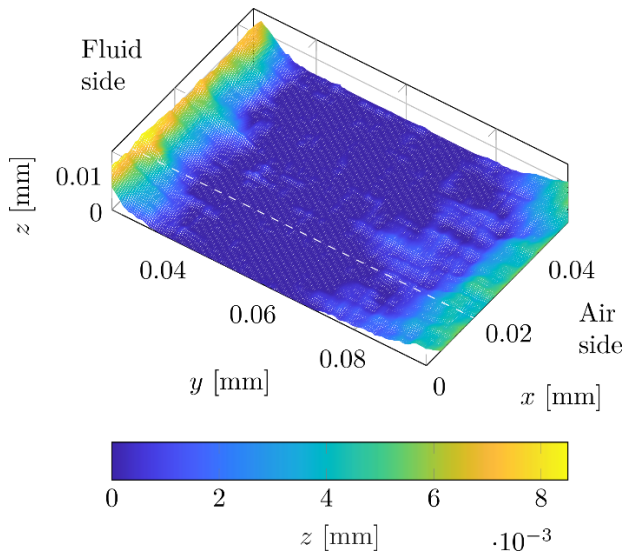


Figure 12. Mounted rough sealing edge

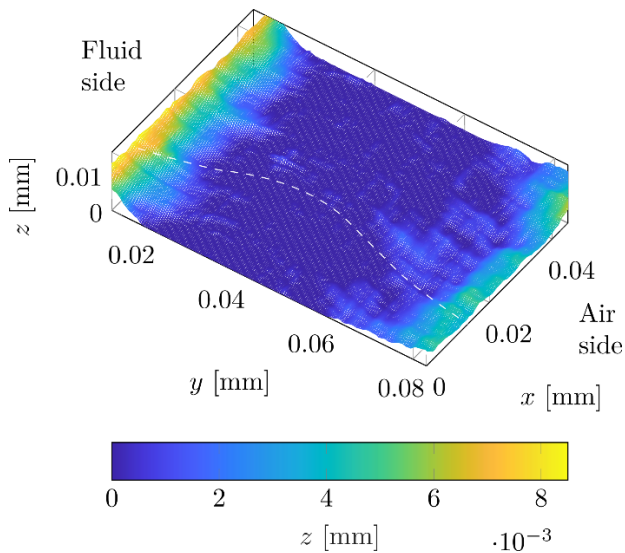


Figure 13. Distorted rough sealing edge

circumferential direction, see Fig. 14. For mounting, the radial lip seal is shifted axially onto the shaft and thus pressed onto the shaft surface. The results are the so-called waves of detachment, better known as Schallamach waves. Schallamach [36] observed the contact between a soft rubber body and a hard glass body. He found that the asperities of the rough rubber surface orientate normal to the direction of movement due to shear stresses and form the waves of detachment. Schulz et al. [11] also observed this effect on radial lip seals through a hollow glass shaft. In Figures 14 and 15 this effect is visible in the pressure distribution. As the shaft starts to rotate, the asperities realign themselves and the pressure distribution is displaced in the circumferential direction. Due to the axially asymmetrical pressure profile, the pressure distribution also displaces asymmetrically in the circumferential direction.

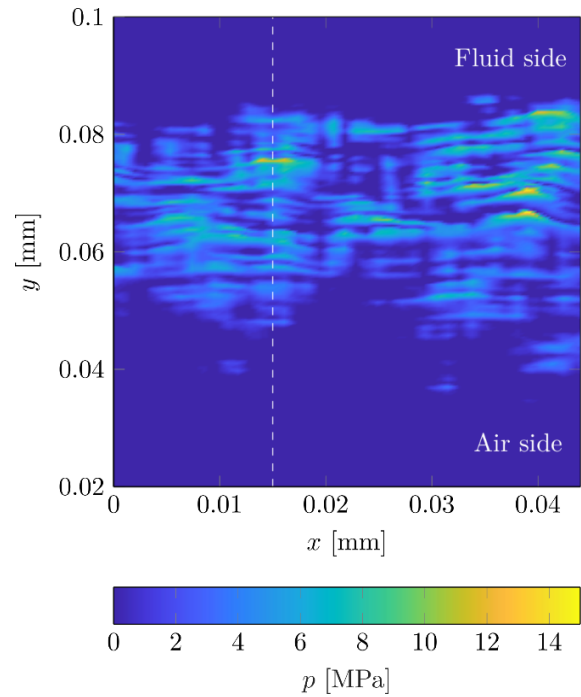


Figure 14. Pressure distribution of the mounted rough sealing edge

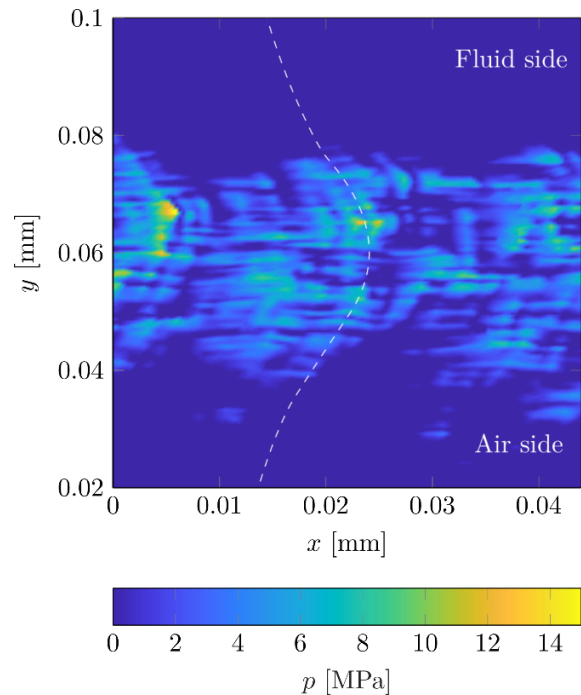


Figure 15. Pressure distribution of the distorted rough sealing edge

In summary, it can be stated that asymmetrically distributed microscopic back-pumping structures are formed by local deformations in the contact area. Furthermore, asymmetrically distributed local pressure differences occur. It is assumed that both effects have a positive influence on the hydrodynamics in the sealing gap. They improve the lubrication and the back-pumping capability of radial lip seals.

4. Summary and conclusion

This paper presents an efficient numerical approach for the structural analysis of radial lip seals. The development of a three-dimensional multiscale model for the simulation of the microscopic processes in the contact area between sealing edge and shaft surface is described in detail. An efficient mesh construction is employed for this purpose. The applied material properties and boundary conditions are presented. A numerical method is used to generate rough sealing edge surfaces. The results offer an insight into the micromechanical contact deformations on radial lip seals. In contrast to previous work, where only the compressed radial lip seal was simulated, this study also analysed the deformations caused by shaft rotation. Thus, tangential distortions of the sealing edge surface in circumferential direction, which could already be observed in optical investigations, could be verified. This allowed the correlation between the pressure distribution and the local tangential deformation in the sealing contact to be established for both ideally smooth and rough surfaces. Thus the sealing edge distortion principle assumed by Kammüller is confirmed numerically. The results obtained can be used for the analysis of hydrodynamic processes in the sealing gap. Consequently, the presented approach provides the basis for a comprehensive study of the lubrication and sealing mechanism of radial lip seals.

Acknowledgement

This paper has been presented at the 10th International Conference on Tribology – BALKANTRIB '20 organized in Belgrade, on May 20-22, 2021.

References

- [1] ISO 6194-1, Rotary Shaft Lip-Type Seals Incorporating Elastomeric Sealing Elements – Part 1: Nominal Dimensions and Tolerances, 2007.
- [2] DIN 3761-1, Rotary Shaft Lip Type Seals for Automobiles; Terms, Formula Symbols, Tolerances, 1984.
- [3] F. Bauer, Federvorgespannte-Elastomer-Radial-Wellendichtungen, Springer Vieweg, Wiesbaden, 2021, DOI: [10.1007/978-3-658-32922-8](https://doi.org/10.1007/978-3-658-32922-8)
- [4] F. Bauer, W. Haas, Radial lip seals – Overview and function, in Proceeding of the 18th International Colloquium Tribology, 10-12.01.2012, Ostfildern, Germany, p. 155.
- [5] M. Kammüller, Zur Abdichtwirkung von Radial-Wellendichtringen, PhD thesis, Universität Stuttgart, Stuttgart, 1986.
- [6] H.K. Müller, Concepts of sealing mechanism of rubber lip type rotary shaft seals, in Proceedings of the 11th International Conference on Fluid Sealing, 08-10.04.1987, Cannes, France, pp. 698-709.
- [7] Y. Kawahara, H. Hirabayashi, A study of sealing phenomena on oil seals, ASLE Transactions, Vol. 22, No. 1, 1979, pp. 46-55, DOI: [10.1080/05698197908982901](https://doi.org/10.1080/05698197908982901)
- [8] Y. Kawahara, M. Abe, H. Hirabayashi, An analysis of sealing characteristics of oil seals, ASLE Transactions, Vol. 23, No. 1, 1980, pp. 93-102, DOI: [10.1080/05698198008982951](https://doi.org/10.1080/05698198008982951)
- [9] J. Grün, S. Feldmeth, F. Bauer, Wear on radial lip seals: A numerical study of the influence on the sealing mechanism, Wear, Vol. 476, 2021, Paper 203674, DOI: [10.1016/j.wear.2021.203674](https://doi.org/10.1016/j.wear.2021.203674)
- [10] H. van Leeuwen, M. Wolfert, The sealing and lubrication principles of plain radial lip seals: An experimental study of local tangential deformations and film thickness, Tribology Series, Vol. 32, 1997, pp. 219-232, DOI: [10.1016/S0167-8922\(08\)70451-6](https://doi.org/10.1016/S0167-8922(08)70451-6)
- [11] M. Schulz, M. Hagmayer, M. Baumann, F. Bauer, Analysis of fluid flow in the sealing gap of radial shaft seals and elastic deformation of the sealing surface, Journal of Tribology, Vol. 143, No. 12, 2021, Paper 122301, DOI: [10.1115/1.4050139](https://doi.org/10.1115/1.4050139)
- [12] M.J.L. Stakenborg, On the sealing mechanism of radial lip seals, Tribology International, Vol. 21, No. 6, 1988, pp. 335-340, DOI: [10.1016/0301-679X\(88\)90110-7](https://doi.org/10.1016/0301-679X(88)90110-7)
- [13] M.J.L. Stakenborg, H.J. van Leeuwen, E.A.M. ten Hagen, Visco-elastohydrodynamic (VEHD) lubrication in radial lip seals: Part 1 – Steady-state dynamic viscoelastic seal behavior, Journal of Tribology, Vol. 112, No. 4, 1990, pp. 578-583, DOI: [10.1115/1.2920301](https://doi.org/10.1115/1.2920301)
- [14] K. Tønder, R. Salant, Non-leaking lip seals: A roughness effect study, Journal of Tribology, Vol. 114, No. 3, 1992, pp. 595-599, DOI: [10.1115/1.2920922](https://doi.org/10.1115/1.2920922)
- [15] R.F. Salant, A.L. Flaherty, Elastohydrodynamic analysis of reverse pumping in rotary lip seals with microundulations, Journal of Tribology, Vol. 116, No. 1, 1994, pp. 56-62, DOI: [10.1115/1.2927046](https://doi.org/10.1115/1.2927046)
- [16] R.F. Salant, A.L. Flaherty, Elastohydrodynamic analysis of reverse pumping in rotary lip seals with microasperities, Journal of Tribology, Vol. 117, No. 1, 1995, pp. 53-59, DOI: [10.1115/1.2830606](https://doi.org/10.1115/1.2830606)

- [17] R.F. Salant, Elastohydrodynamic model of the rotary lip seal, *Journal of Tribology*, Vol. 118, No. 2, 1996, pp. 292-296, DOI: [10.1115/1.2831298](https://doi.org/10.1115/1.2831298)
- [18] R.F. Salant, A.H. Rocke, Hydrodynamic analysis of the flow in a rotary lip seal using flow factors, *Journal of Tribology*, Vol. 126, No. 1, 2004, pp. 156-161, DOI: [10.1115/1.1609486](https://doi.org/10.1115/1.1609486)
- [19] G. Di Benedetto, M. Organisciak, G. Popovici, A. Stijepić, Film thickness prediction of radial lip seal, *FME Transactions*, Vol. 37, No. 2, 2009, pp. 87-90.
- [20] J.F. Wenk, L. Scott Stephens, S.B. Lattime, D. Weatherly, A multi-scale finite element contact model using measured surface roughness for a radial lip seal, *Tribology International*, Vol. 97, 2016, pp. 288-301, DOI: [10.1016/j.triboint.2016.01.035](https://doi.org/10.1016/j.triboint.2016.01.035)
- [21] F. Shi, R.F. Salant, Numerical study of a rotary lip seal with a quasi-random sealing surface, *Journal of Tribology*, Vol. 123, No. 3, 2001, pp. 517-524, DOI: [10.1115/1.1308028](https://doi.org/10.1115/1.1308028)
- [22] D. Liu, S. Wang, C. Zhang, A multiscale wear simulation method for rotary lip seal under mixed lubricating conditions, *Tribology International*, Vol. 121, 2018, pp. 190-203, DOI: [10.1016/j.triboint.2018.01.007](https://doi.org/10.1016/j.triboint.2018.01.007)
- [23] N. Garcia, E. Stoll, Monte Carlo calculation for electromagnetic-wave scattering from random rough surfaces, *Physical Review Letters*, Vol. 52, No. 20, 1984, 1798-1801, DOI: [10.1103/PhysRevLett.52.1798](https://doi.org/10.1103/PhysRevLett.52.1798)
- [24] D. Bergström, J. Powell, A.F.H. Kaplan, The absorption of light by rough metal surfaces – A three-dimensional ray-tracing analysis, *Journal of Applied Physics*, Vol. 103, No. 10, 2008, Paper 103515, DOI: [10.1063/1.2930808](https://doi.org/10.1063/1.2930808)
- [25] S.E. Benzley, E. Perry, K. Merkley, B. Clark, G. Sjaardama, A comparison of all hexagonal and all tetrahedral finite element meshes for elastic and elasto-plastic analysis, in *Proceedings of the 4th International Meshing Roundtable*, 1995, Albuquerque, USA, 179-191.
- [26] Altair HyperMesh 2019 User's Guide, available at: https://2019.help.altair.com/2019/hyperworks/pdf/s/hm/HyperMesh_2019_UserGuide.pdf, accessed: 20.01.2022.
- [27] Marc 2019 Feature Pack 1 Volume A: Theory and user information, MSC.Software Corporation, 2019.
- [28] Marc 2019 Feature Pack 1 Volume B: Element Library, MSC.Software Corporation, 2019.
- [29] S. Feldmeth, F. Bauer, W. Haas, Component-based parameter identification for the contact simulation of elastomeric radial lip seals, in *Proceedings of the Deutsche Kautschuk-Tagung DKT 2015 and International Rubber Conference IRC 2015*, 29.06-02.07.2015, Nuremberg, Germany, p. 194.
- [30] A. Tasora, E. Prati, T. Marin, A method for the characterization of static elastomeric lip seal deformation, *Tribology International*, Vol. 60, 2013, pp. 119-126, DOI: [10.1016/j.triboint.2012.10.025](https://doi.org/10.1016/j.triboint.2012.10.025)
- [31] D.E. Johnston, R. Vogt, Rotary shaft seal friction, the influence of design, material, oil and shaft surface, *SAE Technical Paper Series*, 1995, Paper 950764, DOI: [10.4271/950764](https://doi.org/10.4271/950764)
- [32] T. Engelke, Einfluss der Elastomer-Schmierstoff-Kombination auf das Betriebsverhalten von Radialwellendichtringen [Effect of the elastomer-lubricant-combination to the performance of radial shaft seals], PhD thesis, Gottfried Wilhelm Leibniz Universität Hannover, Hannover, 2011 [in German].
- [33] S. Plath, S. Meyer, V.M. Wollesen, Friction torque of a rotary shaft lip type seal – A comparison between test results and finite element simulation, *Mechanika*, Vol. 54, No. 4, 2005, pp. 55-59.
- [34] S. Feldmeth, M. Stoll, F. Bauer, How to measure the radial load of radial lip seals, *Tribologie und Schmierungstechnik*, Vol. 64, No. 3-4, 2021, pp. 5-12, DOI: [10.24053/TuS-2021-0014](https://doi.org/10.24053/TuS-2021-0014)
- [35] DIN 3761-8, Rotary Shaft Lip Type Seals for Automobiles; Test; Carrying Out Axle-Sections, 1984.
- [36] A. Schallamach, How does rubber slide? *Wear*, Vol. 17, No. 4, 1971, pp. 301-312, DOI: [10.1016/0043-1648\(71\)90033-0](https://doi.org/10.1016/0043-1648(71)90033-0)